Chapter 4

Simulating cone counting systems in Matlab

Now that we have the necessary information and set of concepts for a thorough understanding of the numerical modeling, we will finally delve into the numerical results obtained. It is relevant to mention that we utilized Gullstrand's schematic eye in the simulations. First, we will start by inspecting the optimal configuration of cones in our target area. Then a comprehensive explanation of the coronagraph configuration will be given. At that point, we'll see how it handles a single cone as an input, and what happens when more cones are added to the system. How the configuration increases the resolution of other systems will also be discussed. Finally, the scanning of the cones as they are counted will be modeled and tested numerically.

4.1 The grid

We started this experiment by analyzing the configuration of the cones in the fovea. These densely packed areas have been observed to arrange in an hexagonal grid.

Like squares and equilateral triangles, regular hexagons fit together without any gaps to tile the plane (three hexagons meeting at every vertex), and so are useful for constructing tessellations. The cells of a beehive honeycomb are hexagonal for this reason and because the shape makes efficient use of space and building materials.

The Voronoi diagram of a regular triangular lattice is the honeycomb

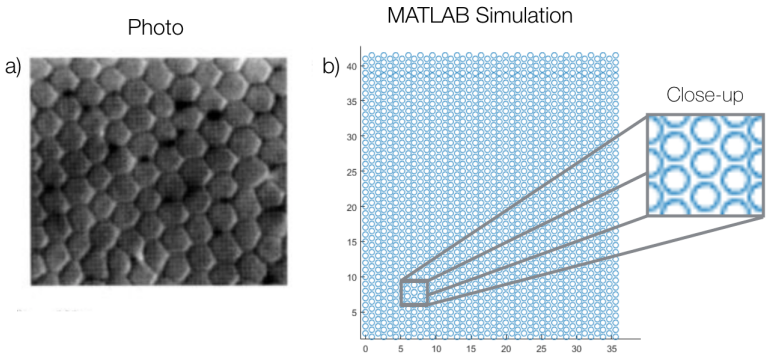

Figure 4.1: a) Photography of densely packed cones in the fovea. The arrangement of the cones appear hexagonal. Photo thanks to (C. a. Curcio et al.). b) Simulation of the spatial distribution of cones in the retina as an hexagonal grid.

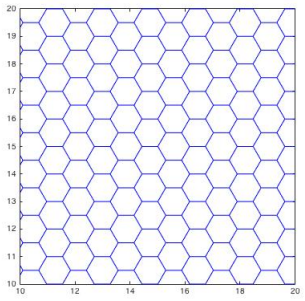

Figure 4.2: a) "Honeycomb" or hexagonal tessellation.

tessellation of hexagons. As a measure of caution, we used a Voronoi diagram to simulate arrangements that are not perfectly hexagonal, with an error of 2% and 4% respectively. We can still see that every cone has six bordering neighbors, which is enough to facilitate the numerical simulations by "seeing" up to 7 cones at a time, and consider the rest of the grid symmetrical.

Each cone produces an Airy pattern, so we model the cone mosaic by arranging this type of patterns in the corresponding array.

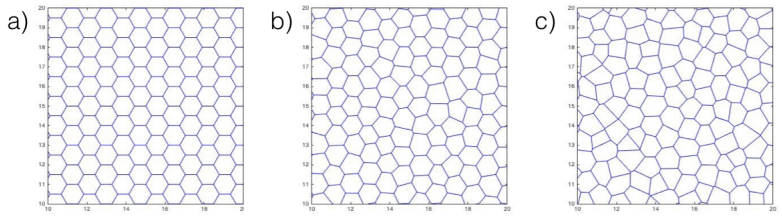

Figure 4.3: Matlab generated Voronoi image of cone distribution in fovea. a)Perfectly hexagonal grid. b) 2% error in distribution. c) 4% error in distribution.

4.2 The coronagraph

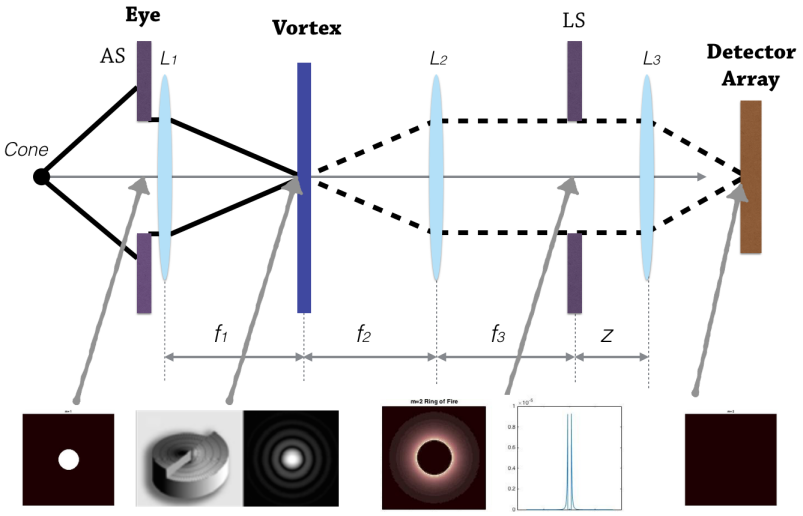

Figure 4.4: Coronagraph to be simulated.

We will be simulating a coronagraph as described in Fig.4.4. The light emitted from the cone exits through the pupil and the lenses and focused in a phase vortex mask. The light is then passed through a lens that changes the wavefront from spherical to planar waves. A Lyot stop filters all the helicoid light resulting from the vortex and on the detector we see nothing.

In terms of the simulation, the fact that the vortex is a fork-hologram or a liquid crystal screen is numerically irrelevant.

Numerically, we can see in in Fig.4.4 the intensity of the resulting light in every step of the way. First, as a top hat, which later becomes a *ring of fire* after passing through the vortex mask. Finally the empty graph in final step shows us that all the light has been filtered by the Lyot stop.

Single cone case

Let's begin by seeing what happens to a single point source whose light passes through the coronagraph. First without the vortex, only lenses and stops; then with a vortex. As we can see in Fig.4.5 there is a "window" created by the phase vortex, where all the light is pushed outwards and a dark spot appears.

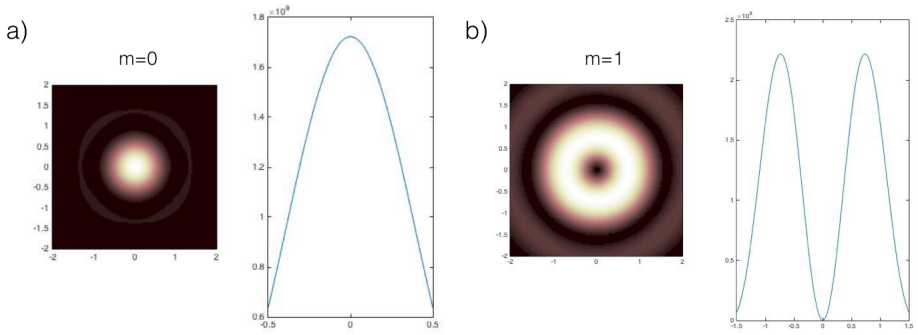

Figure 4.5: The intensity of a single cone with and without a vortex. Note that there is no filtering of the light affected by the vortex yet.

Multiple cones case

We can easily test the cones in different configurations, but as we saw at the beginning of the chapter we know that in the fovea cone cells are arranged in a hexagonal-like grid. Fig.4.6 is a regular hexagon with a vortex placed at the center of the hexagon and with a topological charge of $m = 0, 1, 2, 3$. The results are similar even when the hexagon is not a regular one. We introduced a small random error in Fig.4.7 to test the viability of the method in non-ideal conditions. We account for a possible multilayered structure by varying the intensity of the individual cones, this can be observed in Fig.4.8.

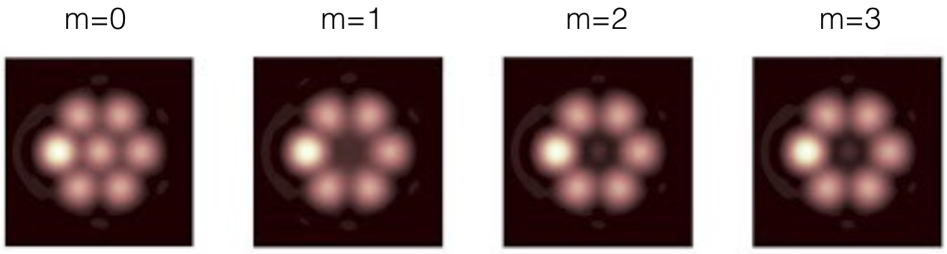

Figure 4.6: 7 cones arranged as a perfect hexagon.

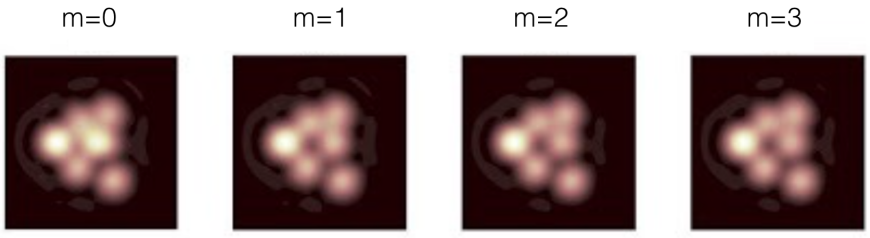

Figure 4.7: 7 cones arranged in an hexagon with a small error.

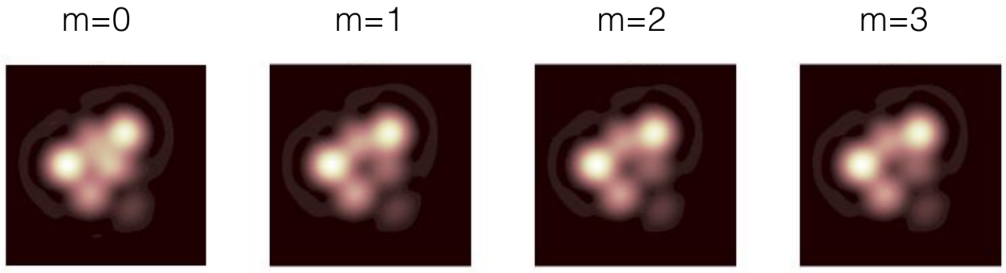

Figure 4.8: 7 cones arranged in an hexagon with a small error and slight varying intensities.

The hexagon simulated is fairly similar to every other hexagon in the tessellation, thus we can consider the arrangement symmetrical enough for the purposes of this text.

4.2.1 Increased resolution

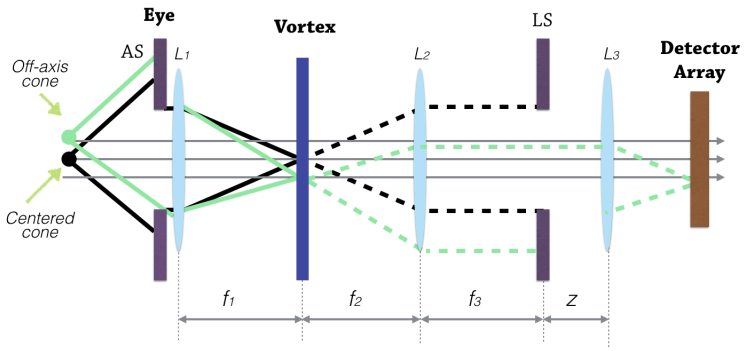

Figure 4.9: A diagram of the optical system with two cones as input.

We now know what, happens to a single point source as it travels through and out our optical system, but what happens to a second point source close to the first one? In Fig.4.9 we will see the results of adding an extra cone off-axis, to the single cone system described in Fig.4.4.

As we saw earlier, the cone that was centered with the axis of the optical system was affected by the vortex; was pushed outwards and thus thoroughly filtered by the last Lyot stop, making possible for the much dimmer light coming from the off-axis cone to be "left alone", in such a way that we can appreciate it without the glare of the centered cone.

Rayleigh Criterion

At this time, it would be necessary to finally explain The Rayleigh Criterion. This "limit" is the generally accepted criterion for the minimum resolvable detail. It quantifies the maximum distance two sources can be before they are no longer resolvable. The imaging process is said to be diffraction-limited when the first diffraction minimum of the image of one source point coincides with the maximum of another. That is the case of our optical system.

If a circular lens is used to observe two point sources, with small angular separation between them, diffraction limits the capability of the system to distinguish those two objects. The criterion to be able to separate two point sources is based on the idea that if the central maximum of the first object

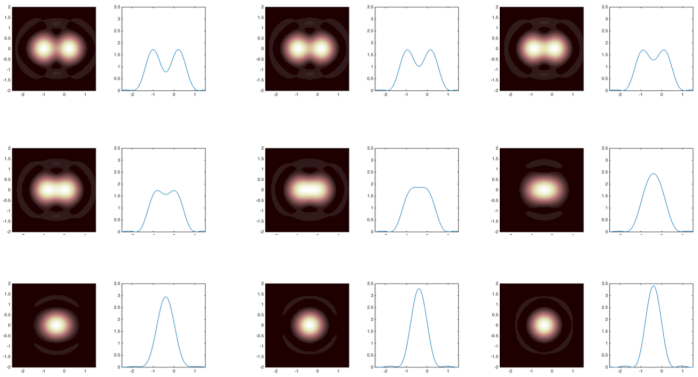

Figure 4.10: 2 cones moving closer to each other show the limits of the Rayleigh Criterion for optical resolution.

is located in the first minimum of diffraction of the second object, the two object can be distinguished. This limit, called **The Rayleigh Criterion** is described mathematically by the expression

$$\theta_R = \sin^{-1}\left(\frac{1.22\lambda}{d}\right) \tag{4.1}$$

where θ_R is the minimal angular separation in radians, λ is the wavelength of the light used to observe the subjects, and d is the diameter of the exit pupil of the system. It is important to mention, that the resolution power of the coronagraph goes beyond the limits established by the Rayleigh Criterion. Experimental test-runs, to identify how much more accurate this new method is, are being conducted in Monterrey by a Visual Optics group at the time of the writing of this text.

Fig.4.11 shows numerical simulations of a two-cone setup with a vortex of topological charge of $m = 1, 2$. Dr Roorda recommends the use of $m = 2$ and explains that it is best to utilize the minimum that appears in the secondary source as a prompt for an automated method of cone counting.

4.3 Scanning

A vital part of simulating an automatic cone counting system is the scanning of the retina. In the process of counting the cones the camera moves at an

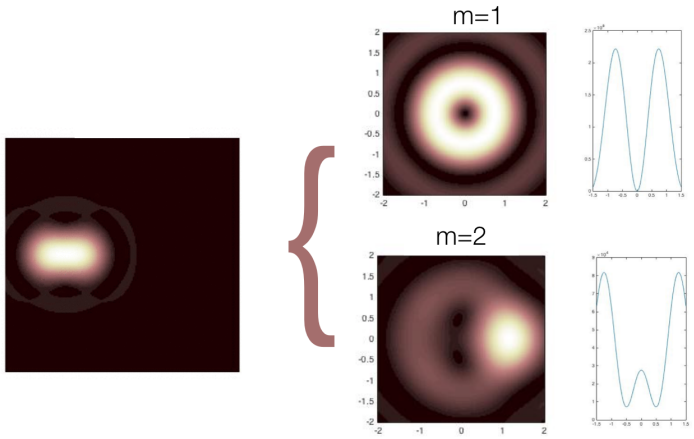

Figure 4.11: To the left: PSF of two cones, To the right:Colormap and profile of two cones, one centered and another off-axis, simulated through the optical system described before.

angle that allows it to sweep the target area of the retina. When the scanning is being performed, what happens numerically is that a growing scalar n is being multiplied with the phase ϕ of the source point. This "shifts" the location of the point in the x axis (or x and y in 2D). We can see in Fig.4.12 how it affects a single cone as it "moves to the right" relative to us. This is as if the camera was the one changing the angle. In the lower images we can see the shift in the profile of the function, while its form remains unchanged.

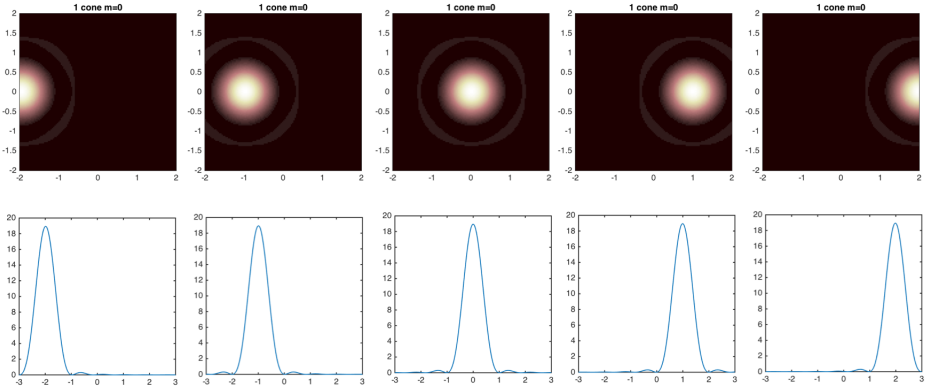

Figure 4.12: PSF of a single cone as it changes its position.

The same happens with two cones, they change positions along the axis as the angle of the camera increases, we can see this phenomena in Fig. 4.13.

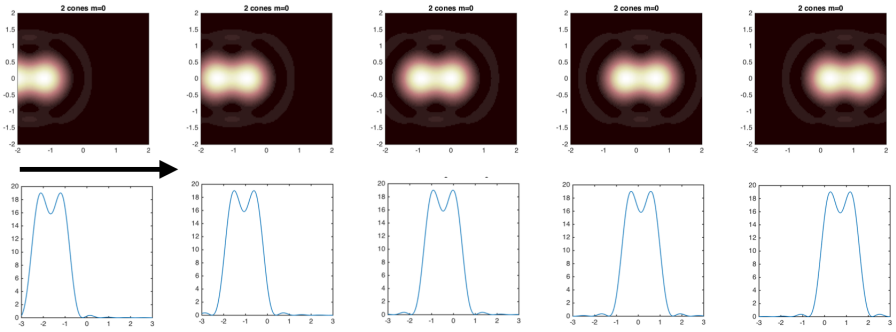

Figure 4.13: "2 cones at 20% of the Rayleigh resolvability distance.

In the hexagonal arrangement similar results can be observed. Fig.4.14 shows 5 frames from the video simulation of the scanning of 7 cones in an hexagon formation.

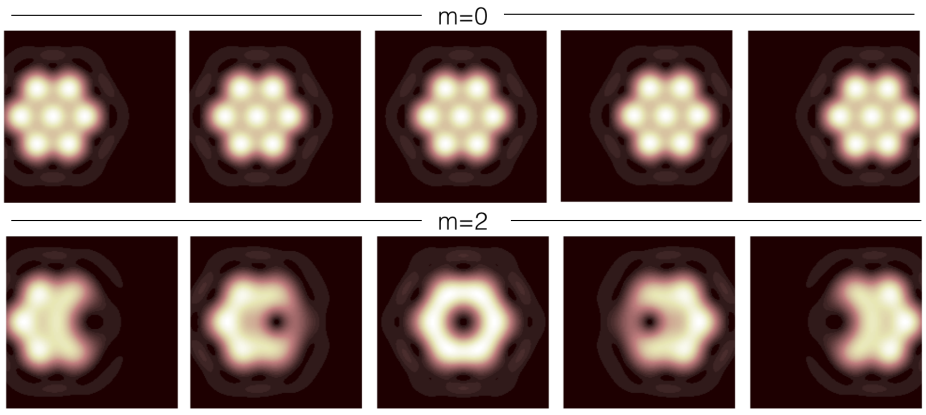

Figure 4.14: "7 cones in a hexagonal arrangement, the scanning is being performed so we see the hexagon "move" to the right relative to us. In the lower images a vortex of m=2 is being used to detect the cones.

Next, we have in Fig.4.15 two cones, at 20% the Rayleigh distance, that are being scanned by a m=2 vortex, we can see the shifts in position and the change in intensity as the vortex interacts with the cones.

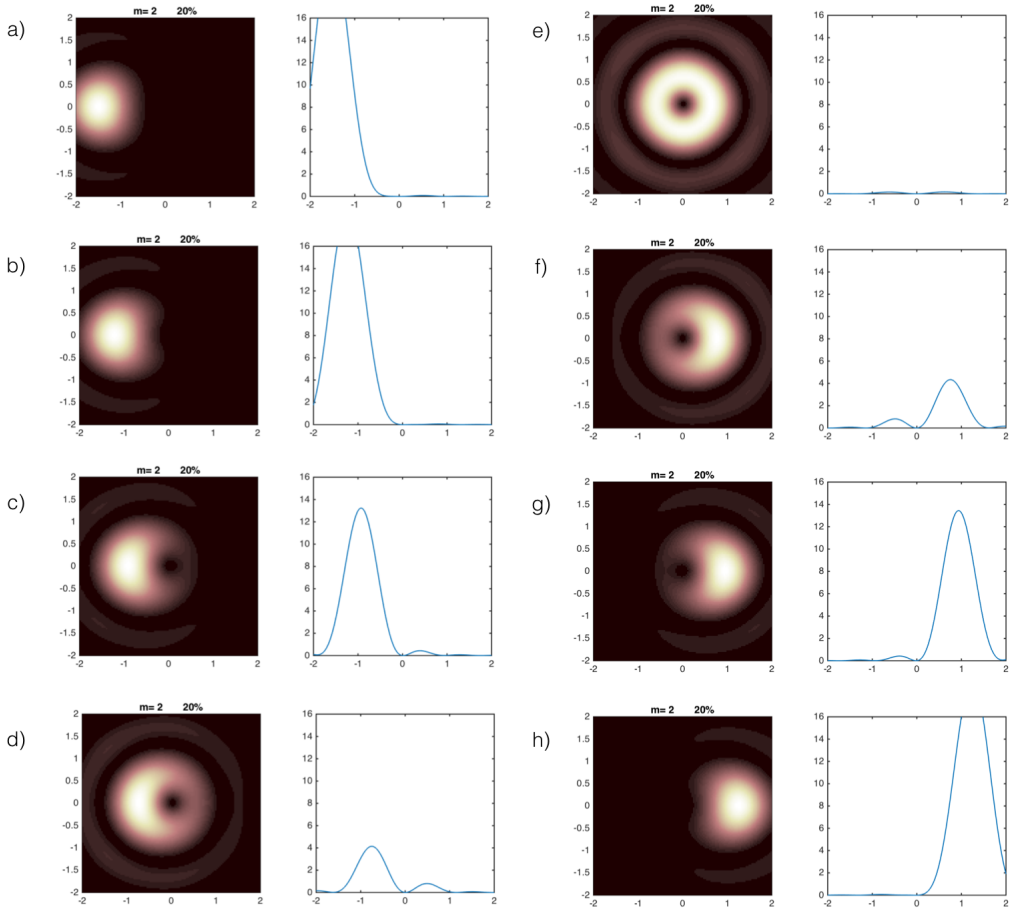

Figure 4.15: "2 cones at 20% of the Rayleigh distance. The scale in this image hinders us from seeing the minima where it actually is.

Nowadays the actual counting of the cones is based on the position of their maxima, we want to change that, so with help of the vortex we can count the minima and be more accurate and fast. Fig.4.3 shows two cones below the Rayleigh distance, and we can see on their profile that when we align one of them with the vortex we can see an intensity minimum close to $x = 0$, were the second cone is located. Not only can we increase the resolvability of the cones. but we can also know exactly how distant they are from each other by observing where the first minimum appears as one of the cones is being completely filtered by the final Lyot stop. For example:

in Fig.4.3 we can see the minimum at 0.2, which means that the cones are separated by a distance of 20% the Rayleigh criterion (Mari et al.).

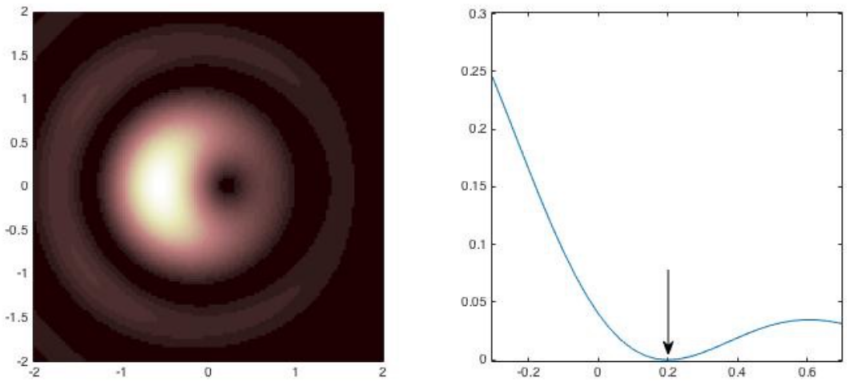

Figure 4.16: 2 cones at 20% of the Rayleigh distance.

The importance of having simulated the scanning system comes from the fact that it is vital for an automatized cone counting method to be developed around our findings. Now that we can detect more accurately how many cones there are, and tell their precise location, it opens a whole lot of potential for the cone counting system to be developed experimentally. This system has been very successfully implemented in astrophysics for exoplanetary detection, and the possibility for it to be used in cone detection is now more feasible than ever.